

Following Single Molecules by Force Spectroscopy

OLGA K. DUDKO,^a ALEXANDER E. FILIPPOV,^b JOSEPH KLAFTER,^c AND MICHAEL URBACH^{c,*}

^aMathematical and Statistical Computing Laboratory, National Institutes of Health, Bethesda, Maryland 20892, USA

^bDonetsk Institute for Physics and Engineering of NASU, 83144, Donetsk, Ukraine

^cSchool of Chemistry, Tel Aviv University, Tel Aviv 69978, Israel

(Received 16 May 2004)

Abstract. Dynamic force spectroscopy of single molecules, in which an adhesion bond is driven away from equilibrium by a spring pulled with velocity V , is described by a model that predicts the distribution of rupture forces (mean and variance), all amenable to experimental tests. The distribution has a pronounced asymmetry, which has recently been observed experimentally. The mean rupture force follows a $(\ln V)^{2.3}$ dependence on the pulling velocity and differs from earlier predictions. Interestingly, at low pulling velocities a rebinding process is observed whose signature is an intermittent behavior of the spring force that delays the rupture. Based on the rupture mechanism, we propose a new “pick-up-and-put-down” method to manipulate individual molecules with scanning probes. We demonstrate that the number of molecules picked up by the tip and deposited at a different location can be controlled by adjusting the pulling velocity of the tip and the distance of closest approach of the tip to the surface.

1. INTRODUCTION

Single molecule spectroscopy is by now an established approach that can report on distributions of molecular properties and can provide kinetic information on conformational changes such as folding and unfolding of molecules without the “scrambling” that occurs due to ensemble averaging.¹ Such information could be valuable in particular for biomolecules, where rare events might have functional significance but can be masked in an ensemble approach. Dynamic force spectroscopy (DFS) has been introduced as a spectroscopic tool to probe the complex relationship among “force-lifetime-and-chemistry” in single molecules bound in an adhesion complex^{2–4} and to reveal hidden details of molecular scale energy landscapes and adhesion strengths. The corresponding experiments probe mechanical forces on small scales and provide a versatile tool for studying molecular adhesion and friction through the response to mechanical stress of single molecules or of nanoscale tips. The probing techniques include atomic force microscopy (AFM),^{2,5} biomembrane force probe microscopy,³ and optical tweezers.⁴ Examples of processes that are investigated are friction on the atomic scale,^{5,8}

specific binding of ligand–receptor,^{9,10} protein unfolding,^{11,12} and mechanical properties of single polymer molecules such as DNA.^{13,14}

The rupture force in DFS is quantified by the maximum extension of a spring, the linker, which is followed by a rapid recoil of the spring to its rest position (see Fig. 1). This resembles the stick-to-slip transition in studies on friction. The unbinding process of a single molecule is studied one molecule at a time, which means that one measures a collection of independent random rupture events. This type of measurement leads to a distribution of rupture forces. In addition, measurements of rupture forces over a wide range of pulling velocities, from very slow to extremely fast, are used to explore the energy landscape of the bound complex. Velocity serves as a main “control” parameter that determines the rupture force.

Understanding unbinding processes on the single-molecule level, and in particular its dependence on the pulling velocity, opens new ways for manipulating individual molecules and for controllable modification of

*Author to whom correspondence should be addressed. E-mail: urbakh@post.tau.ac.il

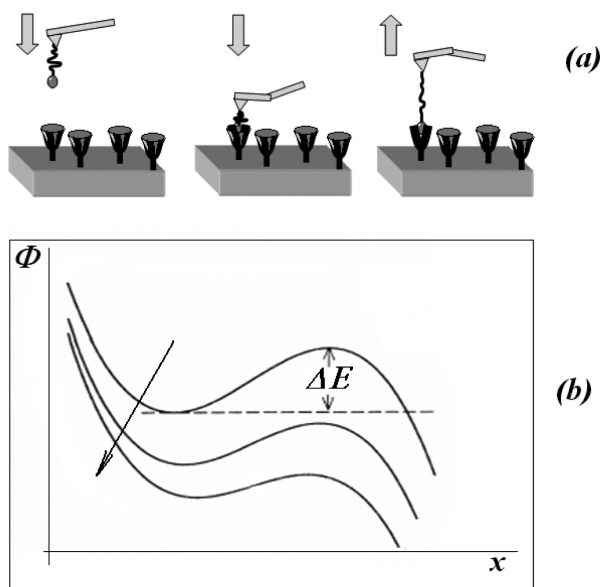


Fig. 1. (a) A schematic presentation of the DFS measurement demonstrating the preparation of the adhesion complex and the pulling away from equilibrium. (b) The total potential experienced by the bond for three different extensions of the spring in the pulling stage. The arrow points in the direction of the growing extension.

surface structures. Manipulation of individual molecules can be used to build new molecular suprastructures, to explore the influence of the environment on a molecule, or to realize and test concepts for new nanodevices.^{15–21} Soon after the invention of scanning tunneling microscopy (STM) and atomic force microscopy (AFM) it was recognized that scanning can alter surface topography. At that time this was considered a drawback for imaging. However, it turned out that these observations led to the idea of controllable modification of surface structure at the atomic scale, which attracted the attention of a large number of research groups.^{15–26} The ability to manipulate individual atoms, molecules, and clusters with scanned probes has opened new fascinating areas of research and allowed the performance of “engineering” operations at the ultimate limits of fabrication.

Manipulations are usually classified into two types: lateral and vertical.^{18–26} In the lateral case an object is displaced (pulled, pushed, or slides) from one position to another along the surface. In the case of vertical manipulation the object is transferred between the surface and the tip. In the literature this mode is sometimes referred to as “pick-up-and-put-down”.¹⁹ Lateral movements of adsorbates have been the subject of numerous

experimental and theoretical studies.^{18,20–23} However, controllable vertical manipulations of individual adsorbates by AFM are just at the beginning.^{18,21,24–28} It is more difficult to control vertical manipulations than lateral ones, since the energy barriers to be overcome when pulling an individual adsorbate off a surface are usually higher than for lateral movements. Here is where the need to understand the unbinding (rupture) enters, which makes the single molecular rupture and the molecular manipulation intimately related.

In the present paper we discuss a new approach²⁹ to describe unbinding processes measured by DFS, which goes beyond previous models and methods of analysis.^{4,30–36} As we show, our approach: (1) proposes a possible mechanism of rupture, (2) emphasizes the importance of investigating the *distribution* function of rupture forces rather than focusing on *typical* rupture forces only, and (3) gives a deeper insight into the effects of rebinding. We also demonstrate that the number of molecules picked up by a tip and deposited at another surface location can be controlled by adjusting the pulling velocity of the tip and the distance of closest approach of the tip to the surface. This differs from an earlier suggestion to control the extraction of atoms from a surface through the duration of maximal stay in the vicinity of the surface.²⁴

2. UNBINDING OF A SINGLE MOLECULE

In DFS experiments an adhesion bond is driven away from its equilibrium by a spring pulled at a given velocity. Rupture of adhesion bonds occurs via thermally assisted escape from the bound state across an activation barrier. The latter diminishes as the applied force increases, so the rupture force is determined by an interplay between the rate of escape in the absence of the external force, and the pulling velocity (loading rate). Thus, the measured forces are not an intrinsic property of the bound complex, but rather depend on the mechanical setup and loading rate applied to the system.

Let us consider a one-dimensional description of the unbinding process along a single reaction coordinate, x . The dynamic response of the bound complex is governed by the Langevin equation

$$M \ddot{x}(t) = -\gamma_x \dot{x}(t) - \frac{\partial U(x)}{\partial x} - K(x - Vt) + \xi_x(t) \quad (1)$$

Here the molecule of mass M is pulled by a linker of a spring constant K moving at a velocity V . $U(x)$ is the adhesion potential, γ_x is a dissipation constant, and the effect of thermal fluctuations is given by a random force $\xi_x(t)$, which is δ -correlated $\langle \xi_x(t) \xi_x(0) \rangle = 2k_B T \gamma_x \delta(t)$. In eq 1 thermal fluctuations are the origin of the distribu-

tion of rupture forces. In a more general case other sources of randomness are possible.

The bound state is defined by the minimum of the total potential

$$\Phi(X, t) = U(x) + \frac{K}{2}(x - Vt)^2$$

In the absence of thermal fluctuations, unbinding occurs when the potential barrier vanishes, i.e., at the instability point where $d^2\Phi(x, t)/dx^2 = 0$, $d\Phi(x, t)/dx = 0$. At this point the measured spring force, $F = K(x - Vt)$, reaches its maximum value $F = F_c$. In the presence of fluctuations the escape from the potential well occurs earlier, and the probability $W(t)$ that a molecule persists in its bound state is defined by Kramers' transition rate³⁷ and can be approximately calculated through the following kinetic equation

$$\frac{dW(t)}{dt} = -\frac{\Omega_1(t)\Omega_2(t)M}{2\pi\gamma_x} \exp[-\Delta E(t)/k_B T] W(t) \quad (2)$$

Here $\Delta E(t)$ is the instantaneous barrier height and $\Omega_{1,2}(t)$ are the effective oscillation frequencies at the minimum corresponding to the bound state and maximum of the combined potential $\Phi(x, t)$. Equation 2 does not take into account rebinding processes. The experimentally measured distribution of rupture forces, $P(F_{\max})$, can be expressed in terms of W as

$$P(F_{\max}) = -\frac{d}{dF_{\max}} W(F_{\max}), \text{ and} \\ \langle F_{\max} \rangle = -\int_0^{\infty} F'_{\max} \left(\frac{d}{dF'_{\max}} W(F'_{\max}) \right) dF'_{\max} \quad (3)$$

As we have already noted above, the rupture force, F_{\max} , is defined as the maximal spring force, $K(x - Vt)$, measured during rebinding process.

Because of the exponential dependence of the unbinding rate on $\Delta E(t)$, we focus on values of F close to the critical force F_c at which the barrier disappears completely. Then the instantaneous barrier height and the oscillation frequencies can be written in terms of the reduced bias,³⁸ $\varepsilon = 1 - F_{\max}/F_c$, as

$$\Delta E(t) = U_c \varepsilon^{3/2}, \quad \Omega_{1,2}(t) = \Omega_c \varepsilon^{1/4} \quad (4)$$

where U_c and Ω_c are the parameters of the bare, unbiased, potential $U(x)$, which is an *information we are after*. See ref 39 for the definitions of U_c , Ω_c and F_c corresponding to Morse potential.

Solution of the kinetic eq 2 with $\Delta E(t)$ and $\Omega_{1,2}(t)$ given by eq 4 leads to the final expressions for $P(F_{\max})$, its mean value $\langle F_{\max} \rangle$, and the variance $\sigma_{F_{\max}}^2 = \langle F_{\max}^2 \rangle - \langle F_{\max} \rangle^2$:

$$\langle F_{\max} \rangle \approx F_c \left\{ 1 - \left(\frac{k_B T}{U_c} \right)^{2/3} \left[\ln \left(\frac{U_c 3\pi\gamma_x K}{k_B T \Omega_c^2 M F_c} V \right) \right]^{-2/3} \right\} \quad (5)$$

$$P(F_{\max}) = P_0 \varepsilon^{1/2} \exp \left\{ -\frac{U_c}{k_B T} \varepsilon^{3/2} - \frac{k_B T \Omega_c^2 M F_c}{U_c 3\pi\gamma_x K V} e^{-\frac{U_c}{k_B T} \varepsilon^{3/2}} \right\} \quad (6)$$

$$\sigma_{F_{\max}}^2 = \frac{2\pi^2}{27} F_c^2 \left(\frac{k_B T}{U_c} \right)^{4/3} \left[\ln \left(\frac{F_c \Omega_c^2 M k_B T}{K V 3\pi\gamma_x U_c} \right) \right]^{-2/3} \quad (7)$$

where P_0 is a normalization constant.

Expression 5 differs essentially from the earlier proposed and often used logarithmic law, $\langle F_{\max} \rangle = \text{const} + (k_B T/\Delta x) \ln[VK/\Delta x/(k_0 k_B T)]$,⁴ where k_0 is the spontaneous rate of bond dissociation, and Δx is a distance from the minimum to the activation barrier of the reaction potential $U(x)$. The logarithmic law has been derived within a Kramers picture for the escape from a well (bound state) assuming that the pulling force produces a small constant bias, which reduces the height of a potential barrier. This is, however, an unlikely regime. As the linker is driven out of the adhesion complex and the bias is ramped up, a bond rupture occurs preferentially when a potential barrier almost vanishes. A similar mechanism has been recently suggested for interpretation of the effect of thermal fluctuations on atomic friction.^{40,41}

Scaling of rupture forces. Equation 5 predicts a universal scaling, independent of temperature, of $(\langle F_c - \langle F_{\max} \rangle)^{3/2}/T$ with $\ln(V/T)$. Figure 2a shows the agreement between numerical calculations using the Langevin eq 1 and the analytical form in eq 5. Over a wide range of pulling velocities the numerical data obtained for three different temperatures collapse on a single straight line when plotted as $(\langle F_c - \langle F_{\max} \rangle)^{3/2}/T$ vs. $\ln(V/T)$. In contrast, when examining the expression $\langle F_{\max} \rangle \propto \ln(V/T)$ the scaling breaks down (see inset to Fig. 2a). The proposed scaling can be tested experimentally for unbinding and has been shown to work in friction experiments.^{5,8} Figure 2b displays numerical results in agreement with the form in eq 6 for the distribution function of rupture forces calculated for a given velocity. We note the non-Gaussian nature of the distribution and its pronounced asymmetry. Such an asymmetry has been reported already for both small molecules⁴² and macromolecules.¹⁴ The width of the distribution is given by $\sigma_{F_{\max}}^2$ and shows a decrease with a decrease in pulling velocity V .

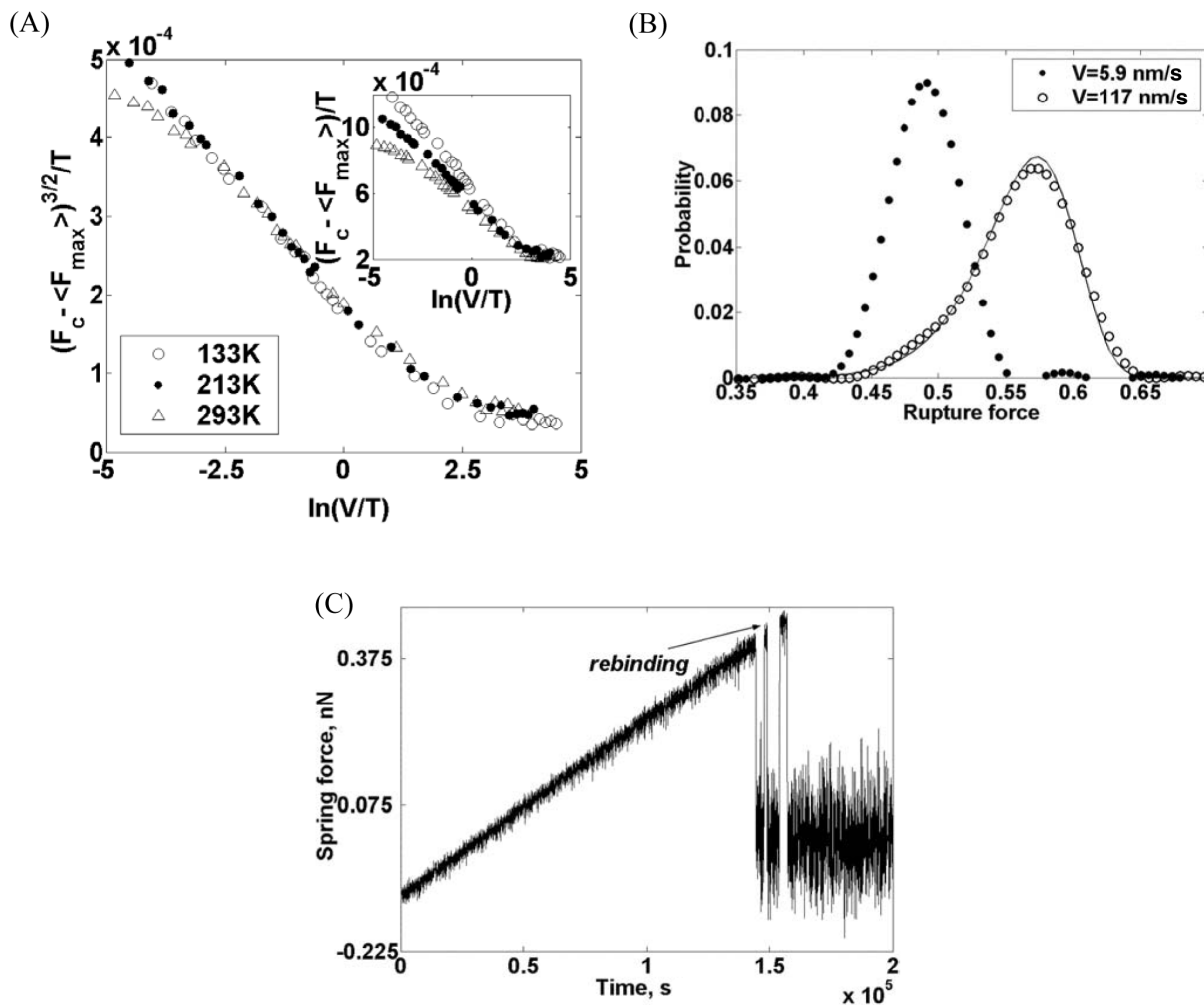


Fig. 2. Analysis of rupture process for a single reaction coordinate. (A) Results of numerical calculations supporting the scaling behavior of the ensemble averaged rupture force according eq 5. The inset shows a significantly worse scaling for the description $\langle F_{\max} \rangle \propto \text{const} - \ln(V/T)$. The units of velocity V are nm/s, temperature is in degrees kelvin. Analyzing the numerical data presented in Fig. 1 gives the following values: $F_c = 0.77$ nN, $U_c = 0.12$ nN nm, and $(U_c 3\pi\gamma_k)/(\Omega_c^2 F_c M) = 6.8 \times 10^{-7}$ nN s. This compares well to the corresponding values of $F_c = 0.75$ nN, $U_c = 0.12$ nN nm, and $(U_c 3\pi\gamma_k)/(\Omega_c^2 F_c M) = 6.8 \times 10^{-7}$ nN s used in our numerical calculations. (B) Normalized distribution of the unbinding force at temperature $T = 293$ K for two values of the velocity. The result from the numerical simulation (solid line) is in a good agreement with the theoretical distribution, eq 6, for velocity $V = 117$ nm/s. For velocity $V = 5.9$ nm/s, where the rebinding plays an essential role, the distribution function deviates from the one given by eq 6. (C) Time series of the spring force showing the rebinding events for $T = 293$ K, $V = 5.9$ nm/s. Parameter values: $K = 0.93$ N/m, $\eta = 7.7 \times 10^{-6}$ kg, $M = 8.7 \times 10^{-12}$ kg, $U_0 = 0.12$ nN \times nm, $R_c = 0.24$ nm, $b = 1.5$.

Our results suggest that fitting experimental data to eqs 5 and 6 one can determine three microscopic parameters of the adhesive potential: F_c , U_c , and $(U_c 3\pi\gamma_k)/(\Omega_c^2 F_c M)$. Thus, DFS experiments can provide new complementary information on adhesive potentials when compared to equilibrium measurements, which provide the spontaneous rate of bond dissociation.

According to Fig. 2a the numerical data at very low and very high pulling velocities deviate from the predicted straight line, $(\langle F_c - \langle F_{\max} \rangle \rangle)^{3/2}/T$ vs. $\ln(V/T)$. The deviation at high driving velocities results from the dominating effect of viscous dissipation given by the term $\gamma_x \dot{x}$ in eq 1, which is not included in the kinetic model, eq 2. The deviation of the unbinding force from

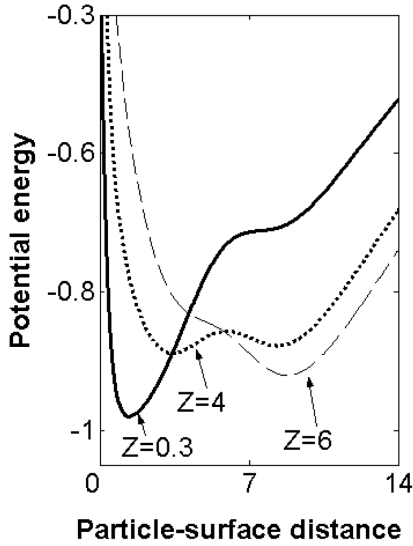


Fig. 3. Schematic presentation of a typical evolution of the effective potential experienced by the molecule with an increase in the tip–surface distance. Parameter values: $U_0^{\text{bulk}}/U_0^{t-m} = 0.1$, $U_0^{\text{surf}}/U_0^{t-m} = 0.05$, $d/R_C^{t-m} = 2$, $L_z/R_C^{t-m} = 6$. Lengths and energy are in units of R_C^{t-m} and U_0^{t-m} respectively.

the analytical form 5 at low pulling velocities is a direct result of rebinding events discussed by Evans,⁴ Seifert,³⁵ and Prechtel et al.,⁴³ and which is clearly observed in the time series of the spring force shown in Fig. 2c. The rebinding appears as an intermittent series resembling stick-slip motion in friction measurements. The deviation of the high temperature curve from scaling in Fig. 2a marks the setting in of rebinding at this temperature.

3. MANIPULATIONS OF INDIVIDUAL MOLECULES BY SCANNING PROBE MICROSCOPY

When a tip is brought into the close vicinity of a surface, the two potential wells corresponding to the equilibrium position of the adsorbate on the tip or on the surface when they are far apart, overlap (see Fig. 3). As a result, the barrier for a transfer of the adsorbate between the surface and the tip decreases. The remaining barrier can be crossed spontaneously due to the presence of thermal fluctuations. However, since the involved relaxation times compete with the moving tip, the adsorbate cannot always follow the motion of the tip, and a probability of the adsorbate transfer between the surface and therefore the tip depends not only on the tip proximity but also on its velocity.

3.1 The Model

In order to mimic the manipulation of adsorbates by scanning probe microscopy, we introduce a model that

consists of a monolayer of N interacting molecules with masses m and coordinates $\mathbf{r}_i = \{x_i, y_i, z_i\}$ located on a substrate, and a tip of mass M and center-of-mass coordinate $\mathbf{R}_i = \{X_i, Y_i, Z_i\}$. The tip is pulled by a spring of stiffness K in the z -direction perpendicular to the surface $\{x, y\}$. The spring is connected to a stage which moves with a constant velocity \mathbf{V} . The dynamics of this system is described by a system of $3N + 3$ equations of motion for the tip and the molecules:

$$M\partial^2\mathbf{R}/\partial t^2 = -\Gamma\partial\mathbf{R}/\partial t - \sum_{i=1}^N\partial U^{t-m}(\mathbf{r}_i - \mathbf{R})/\partial\mathbf{R} - \partial U^{t-s}(\mathbf{R})/\partial\mathbf{R} - K(\mathbf{V}t - \mathbf{R}) \quad (8)$$

$$m\partial^2\mathbf{r}_i/\partial t^2 + \gamma\partial\mathbf{r}_i/\partial t + \partial[U^{t-m}(\mathbf{r}_i - \mathbf{R}) + U^{m-s}(\mathbf{r}_i)]/\partial\mathbf{r}_i + \sum_{j \neq i}^N\partial U^{m-m}(\mathbf{r}_i - \mathbf{r}_j)/\partial\mathbf{r}_j = f_i(t), \quad i = 1, \dots, N \quad (9)$$

Here the potentials U^{m-m} , U^{m-s} , U^{t-m} , and U^{t-s} describe molecule–molecule, molecule–substrate, molecule–tip, and tip–substrate interactions, respectively. The parameters Γ and γ account for the dissipation of the kinetic energy of the tip and each molecule, respectively. The effect of the thermal motion of the adsorbates is given in terms of a random force $f_i(t)$, which is δ -correlated, $\langle f_i(t)f_j(0) \rangle = 2mk_B\gamma T\delta(t)\delta_{ij}$. T is the temperature, k_B is the Boltzmann constant.

In our numerical simulations the molecule–molecule and tip–molecule interactions have been modeled by Morse potentials

$$U^{m-m}(r_i - r_j) = U_0^{m-m} \{ [1 - \exp(-2b^{m-m}(r_i - r_j - R_C^{m-m})/R_C^{m-m})]^2 - 1 \} \quad (10)$$

$$U^{t-m}(R - r_i) = U_0^{t-m} \{ [1 - \exp(-2b^{t-m}(R - r_i - R_C^{t-m})/R_C^{t-m})]^2 - 1 \} \quad (11)$$

while for U^{m-s} and U^{t-s} we used

$$U^{m-s} = \{ U_0^{\text{bulk}} + U_0^{\text{surf}} [\cos(ax) + \cos(ay)] \} \exp[-(z - L_z)^2/d^2] \quad (12)$$

$$U^{t-s} = C_0 \exp[-(Z - L_z)^2/c_0^2] \quad (13)$$

where U_0^{t-m} , b^{t-m} , R_0^{t-m} , U_0^{m-m} , b^{m-m} , R_C^{m-m} are the parameters of the Morse potential. It was also taken into account that the dissipation γ decreases when the molecules move away from the surface, $\gamma(z) = \gamma_0[1 + \exp(-z^2/d^2)]$. It should be emphasized that our further conclusions are mostly independent of the particular forms of the potentials U^{t-m} , U^{m-s} , and U^{t-s} .

3.2 Qualitative Consideration of Nano-Manipulation

Qualitative features of the suggested mechanism of manipulation of individual molecules can be understood within the framework of a simplified one-dimensional model. The model describes a single particle located on the uniform surface and interacting with the tip, which is pulled off the surface with a constant velocity $V = Z = \text{const}$, starting from a height Z_0 . Equations 8 and 9 reduce to a 1D equation of motion for the position of the molecule, z , which under overdamped conditions, $\gamma \gg 1$, reads

$$dz/dZ = -(\partial U_{\text{eff}}/\partial z)/\gamma V \quad (14)$$

Here $U_{\text{eff}} = U^{m-s}(z, Z) + U^{m-t}(z)$ is an effective potential experienced by the molecule due to the surface and the tip. The coordinate Z of the tip enters as a parameter.

Typical evolution of the potential U_{eff} with an increase of tip–surface distance Z is shown schematically in Fig. 3. When the tip and surface are in close contact the two wells corresponding to adsorption on the tip or on the surface overlap, and the resulting U_{eff} can attain the form of an asymmetric single-well. With an increase in the tip–surface distance the effective potential U_{eff} takes the form of a two-well potential, and the barrier between two minima grows.

The set of solutions of eq 14 for different values of Z_0 and V presents trajectories in the coordinates (z, Z) , which give a phase portrait of the dynamical system in the space of parameters of the energy functional $U_{\text{eff}}(z, Z)$. Typical phase portraits are shown in Fig. 4 for four

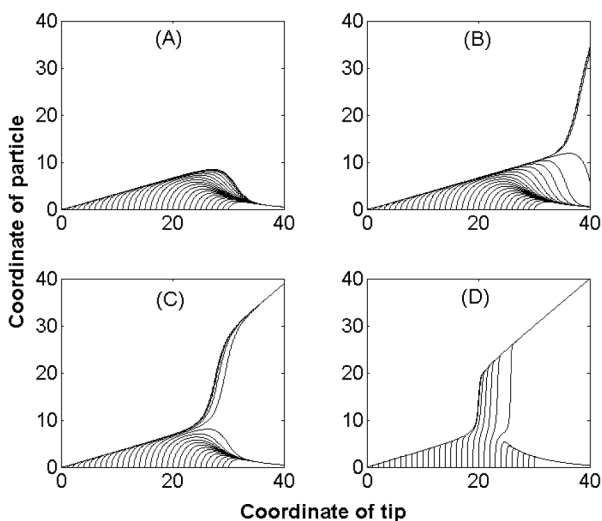


Fig. 4. Trajectories of molecules as a function of the tip coordinates for four values of the pulling velocity: (a) $V = 10$, (b) $V = 9.5$, (c) $V = 7.5$, (d) $V = 0.7$. Parameter values: $U_0^{\text{bulk}}/U_0^{t-m} = 1.9$, $d/R_C^{t-m} = 10$. Lengths and velocities are in units of R_C^{t-m} and $\gamma_0 R_C^{t-m}/m$, respectively.

values of pulling velocities V . All trajectories in Fig. 4 can be separated into two types: (1) trajectories that correspond to a regime where the molecule remains on the surface, and (2) trajectories that belong to a regime in which the tip picks up the molecule and drives it away from the surface. For the first type of trajectories $z \rightarrow z_{\text{ad}}^s$ when $Z \rightarrow \infty$, and for the second type of trajectories $z \rightarrow Z - z_{\text{ad}}^t$ when $Z \rightarrow \infty$, where z_{ad}^s and z_{ad}^t are the molecule–surface and molecule–tip distances for the cases of equilibrium adsorption at the substrate (in the absence of tip) and at the tip (in the absence of substrate), respectively. Figure 4 shows that even being trapped by the tip at small Z , the molecule cannot always follow the tip motion. Due to a finite relaxation time $1/\gamma$ this depends on the tip velocity V . For high pulling velocities the molecule always remains at the surface, independent of the starting tip position, Z_0 (see Fig. 4a). As V decreases, the second type of solutions sets in (Fig. 4 b–d). Furthermore, the starting position of the tip, Z_0 , for which the molecule can still be picked up by the tip increases with a decrease of the pulling velocity.

The above consideration allows one to define the Z_0 -dependent critical velocity of the tip, $V_{\text{cr}}(Z_0)$, that is the maximal V for which the tip drives the particle away from the surface. The result is presented in Fig. 5. For all values of V and Z_0 lying below the curve $V_{\text{cr}}(Z_0)$ the tip does pick up the molecule, and for the values above the curve the molecule does not follow the tip and remains on the surface.

The largest allowed value of the critical velocity can be estimated analytically. In order to do this we consider a motion of the molecule that is trapped by the tip, and assume that the distance between the molecule and the tip remains constant, $z_* = Vt - z(t) = \text{const}$, when the tip is driven away from the surface. In this regime an effective potential experienced by the molecule is dominated by the attraction to the tip and it can be approximated by $U_{\text{eff}} \approx \mathcal{E} \exp[-(z-Vt)^2/\sigma^2]$. Under these conditions the equation of motion (eq 14) leads to the following relation between z_* and V :

$$1 - (\mathcal{E}/\gamma V) z_* \exp(-z_*^2/\sigma^2) = 0 \quad (15)$$

Equation 15 has a solution only for $-z_* < \sigma/\sqrt{2}$ and $V < V_{\text{cr}}^* = \mathcal{E}\sigma/(\gamma\sqrt{2}e)$. For $V > V_{\text{cr}}^*$ the molecule cannot follow the tip motion and remains at the surface. Thus $V = V_{\text{cr}}^*$ is the maximal driving velocity for which the tip can pick up the molecule. The estimated value of V_{cr}^* is in good agreement with the numerical results presented in Fig. 5.

The dependence $V_{\text{cr}}(Z_0)$ not only gives a clue of how to manipulate single molecules but also allows one to estimate a range of tip velocities for which the tip picks up a desirable number, N_n , of molecules when it is

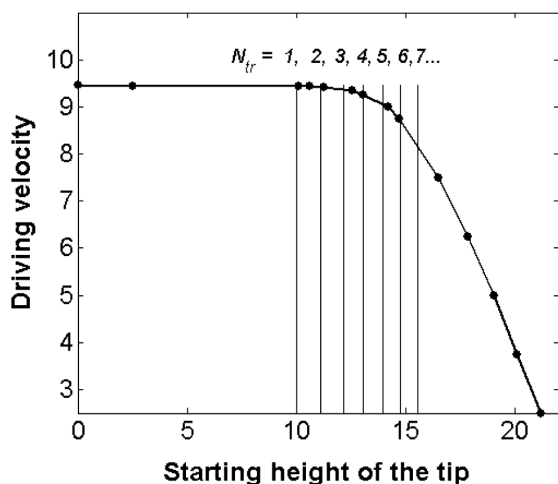


Fig. 5. Maximal velocity for which the tip still drives a particle away vs. starting height of the tip. For all values V and Z_0 below the curve $V_{cr}(Z_0)$ the tip picks the molecule up, while for the values above the curve the molecule remains on the surface. Intersections of the curve $V_{cr}(Z_0)$ with vertical lines give maximal tip velocity for which the tip picks up a given number of particles, $N_{tr} = 1, 2, \dots, 7$ when driven from starting height Z_0 . Parameter values: as in Fig. 3.

driven away starting at the distance $Z = Z_0$. In order to do this we define a function $Z_{cr}(V)$ that gives the maximal value of the initial tip–surface distance for which the tip can trap the molecule being driven away with a velocity V . The function $Z_{cr}(V)$ is the reciprocal of the function $V_{cr}(Z_0)$. Using this information we can conclude that the tip will pick up all molecules located under the tip within a circle of the radius $R = \sqrt{Z_{cr}^2(V) - Z_0^2}$ (Fig. 6). Here we assumed that molecules are distributed uniformly on the surface and do not interact among themselves. Taking into account that $R \propto \delta \sqrt{N_{tr}}$, where δ is an average distance between adsorbates on the surface and N_{tr} is the number of molecules located within the circle, we obtain the following relation between a pulling velocity and the number of molecules picked up by the tip

$$Z_{cr}(V) = \sqrt{Z_0^2 + \delta^2 N_{tr}} \quad (16)$$

Thus intersections of the curve $V_{cr}(Z_0)$ with vertical lines $Z = \sqrt{Z_0^2 + \delta^2 N_{tr}}$ for $N_{tr} = 1, 2, 3, \dots$, which are shown in Fig. 5, give the maximal tip velocity for which the tip picks up a given number of particles, N_{tr} , when it is driven away from the surface starting at distance Z_0 .

It should be noted that the range of tip velocities suitable for controllable molecular manipulation strongly depends on the interaction of the tip with the

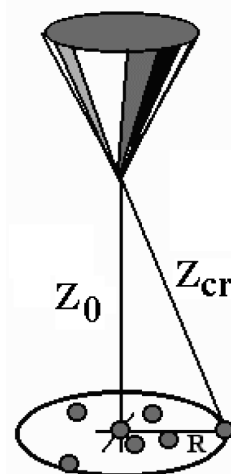


Fig. 6. Schematic explanation to the analytical estimation of the critical velocity V_{cr} : the tip picks up all the molecules located under the tip within a circle of radius R .

molecules. The latter can be made adjustable by modifying the tip chemically.⁴⁴ In this way the critical velocity can be moved into the desirable range. Surprisingly, the characteristic time to extract a molecule has been found to be as slow as 10 ms,²⁴ a time that allows the tip velocity to act as a control parameter.

The same mechanism of manipulation by adjusting the tip velocity and the distance of the closest approach to the surface can be used for deposition of a given number of molecules on the surface. Below we illustrate the proposed mechanism of the pick-up-and-put-down mode of manipulation by numerical simulations.

3.3 Results of the Simulation and Discussion

We have performed numerical simulations of eqs 8 and 9 that describe the coupled dynamics of the externally driven tip and the monolayer of adsorbed molecules. Solving the equations, we started from the equilibrium configuration produced when the tip is brought into close contact with the surface. Then the tip was pulled away from the surface by the spring with a constant velocity. The number of molecules picked up by the tip has been found repeatedly. As a result, we obtained a map of probability to trap a given number of particles by the tip at a given driving velocity, which is presented in Fig. 7. Regions of high and low probability are displayed by red and blue colors, correspondingly. Figure 7b presents the distribution functions of the number of trapped particles for three representative velocities. The map shows that the number of molecules picked up by the AFM tip can vary over a wide range; for the parameters used here this number varies from 0

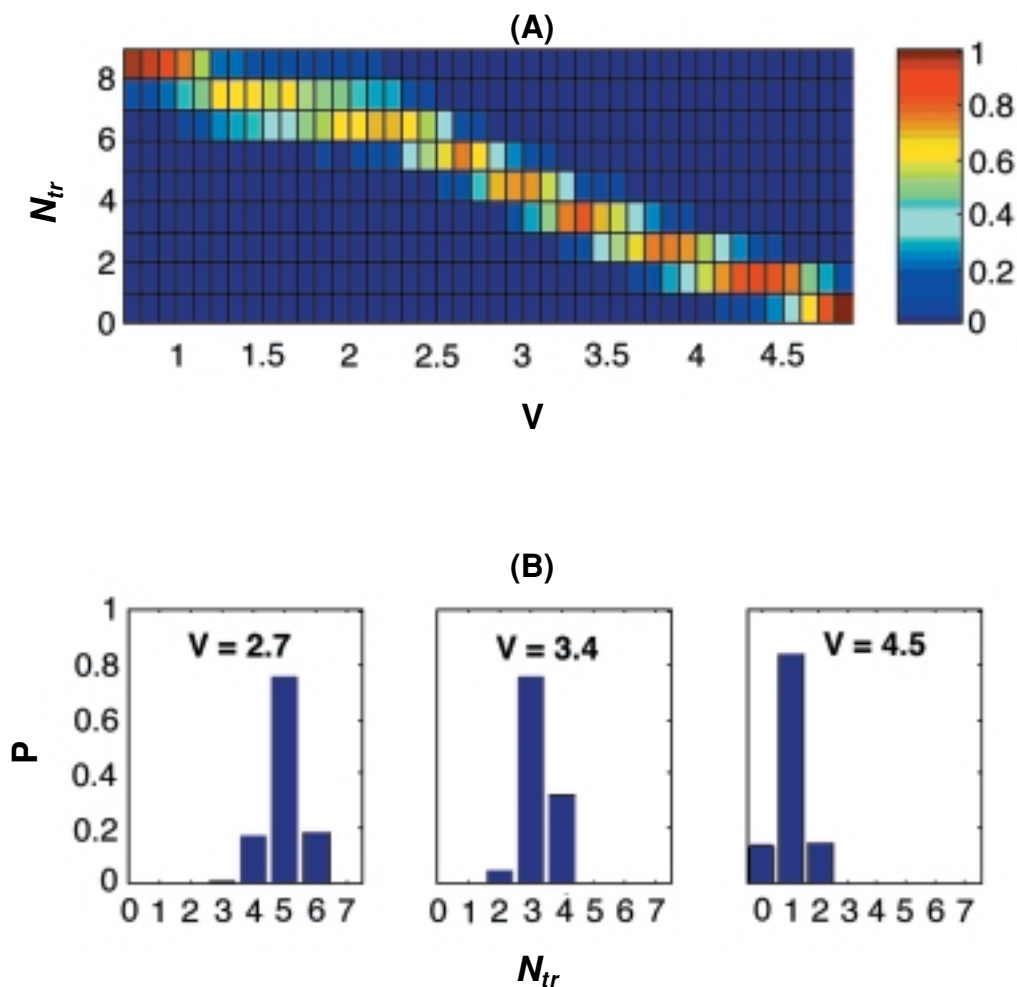


Fig. 7. (a) Probability map, giving the probability to trap a given number of particles at a given driving velocity of the tip. The bar to the right of the map sets up a correspondence between colors and the probability $P(N_{tr}, V)$. (b) Histograms for number of trapped particles corresponding to three values of velocity. Parameter values: $N = 100$, $M = 30m$, $\Gamma = 30\gamma_0$, $a/R_C^{t-m} = 6.3$, $l_z/R_C^{t-m} = 2$, $d/R_C^{t-m} = 1$, $K R_C^{t-m}/U_0^{t-m} = 4.7$, $U_0^{n-m}/U_0^{t-m} = 0.07$, $b^{m-m} = 6$, $R_C^{n-m}/R_C^{t-m} = 1$, $U_0^{bulk}/U_0^{t-m} = 0.7$, $U_0^{surf}/U_0^{t-m} = 0.05$, $C_0/U_0^{t-m} = 0.8$, $c_0/R_C^{t-m} = 2$, $L_z/R_C^{t-m} = -2$, $k_B T/U_0^{t-m} = 10^{-3}$. Lengths and velocities are in units of R_C^{t-m} and $\gamma_0 R_C^{t-m}/m$, respectively.

to 8. The desirable number can be achieved by tuning the driving velocity. In accordance with the qualitative picture discussed above, the number of trapped molecules decreases with the increase in the driving velocity.

It should be noted that not all possible numbers of molecules can be trapped with equal probability. The probability map demonstrates that there are “preferred” numbers of molecules (1, 3, 5, 8) that can be picked up with a high probability, while trapping of 4, 6, and 7 molecules is less probable. The origin of such “magic numbers” can be explained by analyzing molecular configurations that can be formed around the tip. Figure 8 presents examples of the energetically preferred con-

figurations that have been observed in the simulations: five particles (four in a plane and the fifth atop the tip, Fig. 8a), and eight particles (six form hexagonal structure with the tip and two compensate an asymmetry caused by the difference in size of the particles and the tip, Fig. 8b). We remark that the shape of these configurations and the number of particles in them are not universal. They are determined by the radius of the tip and parameters such as molecule–tip and molecule–molecule interactions.

The map shows that the changing of the pulling velocity indeed allows one to control the number of molecules transferred from the adsorbed layer to the tip.

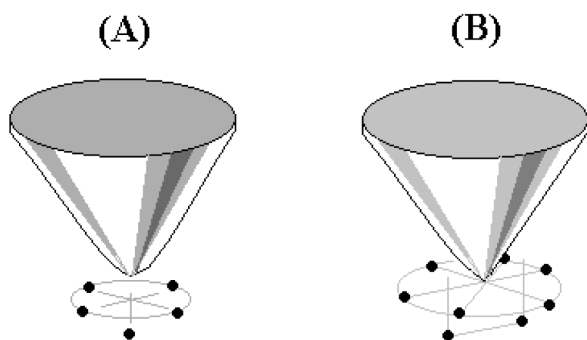


Fig. 8. Examples of preferred configurations formed by the molecules around the tip: (a) five particles (four in a plane and the fifth atop the tip); (b) eight particles (six form a hexagonal structure with the tip and two compensate an asymmetry caused by the difference in size of the particles and the tip).

The proposed manipulation can be optimized and further controlled by adjusting the distance of the closed approach of the tip to the surface and a waiting time before the pulling out of the surface.

4. CONCLUSIONS

In summary, we have shown that single molecules could be followed and manipulated using time-dependent forces. DFS has been investigated in detail, leading to a new dependence of the mean rupture force on the pulling velocity and to an analytical expression for the distribution of rupture forces. In DFS measurements the aim should be obtaining the distribution of rupture forces, since the mean value does not always provide meaningful information about the mechanism of rupture. In particular, when the rupture involves more than a single unbinding path the distribution can have a rich behavior which is not monotonous and cannot be characterized by looking just at the mean.^{10,29} The role of velocity in the DFS is shown to be similar to what is observed in the manipulation of molecules. We therefore propose the velocity as a control parameter in the pick-up-and-put-down of a desirable number of molecules or atoms using scanning probe microscopy.

Acknowledgments. Financial support of this work by the Israel Science Foundation (Grant No. 573/00) and by a grant from ExxonMobil is greatly appreciated. A.E.F acknowledges the support of the Sackler chair for visiting scientists at TAU.

REFERENCES AND NOTES

- (1) Frontiers in Chemistry: Single Molecules (Various authors), *Science* **1999**, 283 (5408, 12 March): 1667–1695.
- (2) Rief, M.; Gautel, M.; Oesterhelt, F.; Fernandez, J.M.; Gaub, H.E. *Science* **1997**, 276, 1109.
- (3) Kellermayer, M.S.; Smith, S.B.; Granzier, H.L.; Bustamante C. *Science* **1997**, 276, 1112.
- (4) Evans, E. *Annu. Rev. Biophys. Biomol. Struct.* **2001**, 30, 105.
- (5) He, M.Y.; Blum, A.S.; Overney, G.; Overney, R.M. *Phys. Rev. Lett.* **2002**, 88, 154302; Stills, S.; Overney, R.M. *Phys. Rev. Lett.* **2003**, 91, 095501.
- (6) Merkel, R.; Nassoy, P.; Leung, A.; Ritchie, K.; Evans, E. *Nature* **1999**, 397, 50.
- (7) Mehta, A.D.; Rief, M.; Spudich, Y.A.; Smith, D.A.; Simmons, R.M. *Science* **1999**, 2831, 689.
- (8) Gnecco, E.; Bennewitz, R.; Gyalog, T.; Loppacher, Ch.; Bammerlin, M.; Meyer, E.; Güntherodt, H.-J. *Phys. Rev. Lett.* **2000**, 84, 1172; Riedo, E.; Grecco, E.; Bennewitz, R.; Meyer, E.; Brune, H. *Phys. Rev. Lett.* **2003**, 91, 084502.
- (9) Florin, E.-L.; Moy, V.T.; Gaub, H.E. *Science* **1994**, 264, 415.
- (10) Nevo, R.; Stroh, C.; Kienberger, F.; Kaftan, D.; Brumfeld, V.; Elbaum, M.; Reich, Z.; Hinterdorfer, P. *Nat. Struct. Biol.* **2003**, 10, 553
- (11) Oberhauser, A.F.; Marszalek, P.E.; Erickson, H.P.; Fernandez, J.M. *Nature* **1998**, 393, 181.
- (12) Carrion-Vazquez, M.; Oberhauser, A.F.; Fowler, S.B.; Marszalek, P.E.; Broedel, S.E.; Clarke, J.; Fernandez, J.M. *Proc. Natl. Acad. Sci. U.S.A.* **1999**, 96, 3694.
- (13) Lee, G.U.; Chrisey, L.A.; Colton, R.J. *Science* **1994**, 266, 771.
- (14) Strunz, T.; Oroszlan, K.; Schäfer, R.; Güntherodt, H.-J. *Proc. Natl. Acad. Sci. U.S.A.* **1999**, 96, 11277.
- (15) Eigler D.M.; Schweizer E.K. *Nature* **1990**, 344, 524.
- (16) Eigler D.M.; Lutz C.P.; Rudge, W.E. *Nature* **1991**, 352, 600
- (17) Avouris, Ph. *Acc. Chem. Res.* **1995**, 28, 95.
- (18) Gimzewski, J.K.; Joachim, Ch. *Science* **1999**, 283, 1683.
- (19) Nyffenegger, R.M.; Penner, R.M. *Chem. Rev.* **1997**, 97, 1195.
- (20) Joachim, C.; Gimzewski, J.K.; Aviram, A. *Nature* **2000**, 408, 54.
- (21) Gauthier, S. *Appl. Surf. Sci.* **2000**, 164, 84.
- (22) Meyer, G.; Zophel, S.; Rieder, K.H. *Appl. Phys. Lett.* **1996**, 69, 3185; *Phys. Rev. Lett.* **1996**, 77, 2113.
- (23) Jung, T.A.; Schlittler, R.R.; Gimzewski, J.K.; Tang, H.; Joachim, C. *Science* **1996**, 271, 181.
- (24) Dujardin, G.; Mayne, A.; Robert, O.; Rose, F.; Joachim, C.; Tang, H. *Phys. Rev. Lett.* **1998**, 80, 3085.
- (25) Oyabu, N.; Custance, O.; Yi, I.; Sugawara, Y.; Morita S. *Phys. Rev. Lett.* **2003**, 90, 176102.
- (26) Buldum, A.; Ciraci, S. *Phys. Rev. B* **1996**, 54, 2175.
- (27) Ben-Ali, M.; Ondarcuhu, T.; Brust, M.; Joachim, C. *Langmuir* **2002**, 18, 872.
- (28) Dudko, O.K.; Filippov, A.E.; Klafter, J.; Urbakh, M. *Nano Lett.* **2003**, 3, 795.
- (29) Dudko, O.K.; Filippov, A.E.; Klafter, J.; Urbakh, M. *Proc. Natl. Acad. Sci. U.S.A.* **2003**, 30, 11378.
- (30) Bell, G.I. *Science* **1978**, 200, 618.

- (31) Grubmüller, H.; Heymann, B.; Tavan, P. *Science* **1996**, *271*, 997.
- (32) Heymann, B.; Grubmüller, H. *Phys. Rev. Lett.* **2000**, *84*, 6126.
- (33) Hummer, G.; Szabo, A. *Proc. Natl. Acad. Sci. U.S.A.* **2001**, *98*, 3658.
- (34) Rief, M.; Fernandez, J.M.; Gaub, H.E. *Phys. Rev. Lett.* **1998**, *81*, 4764.
- (35) Seifert, U. *Europhys. Lett.* **2002**, *58*, 792.
- (36) Bartolo, D.; Derényi, I.; Ajdari, A. *Phys. Rev. E* **2002**, *65*, 051910.
- (37) Hänggi, P.; Talkner, P.; Borkovec, M. *Rev. Mod. Phys.* **1990**, *62*, 251.
- (38) Garg, A. *Phys. Rev. B* **1995**, *51*, 15592.
- (39) In the case of Morse potential, $U(x) = U_0\{[1 - \exp(-2b(x-R_c)/R_c)]^2 - 1\}$ used here for illustration in numerical calculations, we have: $F_c = bU_0/R_c$, $U_c = U_0(1 - 3KR_c^2/(4U_0b^2))^{-1/2}$, $\Omega_c = 2bU_0^{1/2}/(R_cM^{1/2})(1 - 3KR_c^2/(4U_0b^2))^{1/4}$.
- (40) Dudko, O.K.; Filippov, A.E.; Klafter, J.; Urbakh, M. *Chem. Phys. Lett.* **2002**, *352*, 499.
- (41) Sang, Y.; Dube, M.; Grant, M. *Phys. Rev. Lett.* **2001**, *87*, 174301.
- (42) Grandbois, M.; Beyer, M.; Rief, M.; Clausen-Schaumann, H.; Gaub, H. *Science* **1999**, *283*, 1727.
- (43) Prechtel, K.; Bausch, A.R.; Marchi-Artzner, V.; Kantelechner, M.; Kessler, H.; Merkel, R. *Phys. Rev. Lett.* **2002**, *89*, 028101.
- (44) Wong, S.S.; Joselevich, E.; Woolley, A.T.; Cheung, C.L.; Lieber, C.M. *Nature* **1998**, *94*, 52.